SODIUM-CONDUCTING CHANNELS IN CARDIAC MEMBRANES IN LOW CALCIUM

Renzo Levi and Louis J. DeFelice

Department of Anatomy and Cell Biology, Emory University School of Medicine, Atlanta, Georgia 30322

ABSTRACT With no Ca in the patch electrode, two kinds of channels conduct Na in spontaneously beating embryonic chick heart cells. One channel conducts Na primarily during the upstroke of the action potential and is blocked by tetrodotoxin (TTX). The other channel conducts Na primarily during the late plateau and early repolarization phase of the action potential, but only in Ca concentrations below 10^{-6} M. This second channel is TTX-insensitive and has a conductance of 50 to 90 pS, depending upon the interpretation of open-channel flickering. These two Na-conducting channels correspond to the channels that normally carry the fast Na current (I_{Na}) and the slow Ca current (I_{si}).

INTRODUCTION

Single-cell preparation and the patch-clamp technique allow the study of single-channel activity during the action potential in heart cells (Fischmeister et al., 1984). Single-channel recording facilitates the manipulation of one channel, while the rest of the channels in the cell function normally. Using these techniques we have studied Ca channels conducting Na in zero external Ca.

The Ca channel is difficult to observe under normal conditions because its single-channel conductance is low in normal Ca (Cavalie et al., 1983). Here we report that in spontaneously beating chick embryo heart cells, the Ca channel has a large single-channel conductance for Na in the absence of external Ca. The finding that monovalent cations pass through Ca channels under certain conditions emphasizes the results of other investigations: (*a*) Reducing Ca to levels below 10^{-6} M lengthens the action potential. The plateau of these long action potentials, which may last several seconds, lies near the Na equilibrium potential (Hoffman and Suckling, 1956; Rougier et al., 1969; Garnier et al., 1969). (*b*) In voltage-clamp experiments, large inward currents occur in the absence of external Ca in skeletal muscle, (Almers et al., 1984*a, b*), in cardiac muscle (Hess and Tsien, 1984; Hess et al., submitted for publication), in neurons (Kostyuk and Krishtal, 1977*a, b*; Kostyuk et al., 1983), and in mouse neoplastic lymphocytes (Fukushima and Hagiwara, 1985). Na or Li carry these inward currents; however, the kinetics are too slow to implicate I_{Na} channels. Ca channel blockers, like nifedipine, inhibit these monovalent cation currents, but Na channel toxins, like tetrodotoxin (TTX), do not.

In low external Ca, Na ions pass through two kinds of channels in spontaneously beating embryonic chick heart, one of which is unavailable to Na in normal external Ca. In this second category of Na-conducting channel, Na moves inward during the late plateau and early repolarization phase of the cardiac action potential. The channel's conductance is 50–90 pS in 200 mM Na, depending on the interpretation of open-channel flickering (see Results). The channel is insensitive to TTX, and it is inaccessible to Na for Ca concentrations above 10^{-5} M. The channel is not the I_{Na} channel, which we also observe in zero Ca, but is a slower Na-conducting channel with a larger single-channel conductance. The channel is, most likely, the I_{si} channel conducting Na in zero Ca, an interpretation consistent with recent theories of Ca channel selectivity, recent voltage-clamp data, and early action potential data. A preliminary report of this work appeared in the 8th Congress of the International Union of Pure and Applied Biophysics (Levi and DeFelice, 1984).

METHODS

Preparation of chick embryonic ventricular cells by enzymatic digestion of 7-d hearts follows DeHaan (1967). Cells remain in tissue culture medium for 12–24 h on Petri dishes, where they form small rounded clusters (20–40 μm diam) of 2–20 electrically coupled cells. Washing the culture shortly before the experiments in physiological solution (130 Na, 3.5 K, 1.5 Ca, 0.5 Mg, 2 H$_2$PO$_4$, 1 SO$_4$, 135.5 Cl, 5 dextrose, 10 Hepes, and pH 7.3) maintains the cells for hours at room temperature. We use Sylgard-coated, borosilicate glass microelectrodes (model 7052; Corning Glass Works, Medfield, MA, ~2 μm tip diameter before fire polishing). We use 133 mM or 200 mM NaCl in the patch electrode with either 5 mM EGTA or 3 mM EDTA 0 Ca). Assuming that our Ca-free solution, before adding EGTA or EDTA, contains 10^{-5} M Ca, the final concentration of Ca in the pipette solution is 3×10^{-10} M for 5 EGTA and 2.7×10^{-7} M for 3 EDTA. Hepes buffer maintains the pipette solution at pH 7.0. In some experiments, we add 10^{-5} gm/ml TTX to the pipette solution. One electrode (containing the Na and the Ca chelator) records single-channel currents in the cell-attached configuration. A downward deflection indicates an inward current. A second electrode (containing an intracellular-like solution) records action potentials in the whole-cell configuration. Alternatively, we obtain action potentials at the end of a cell-attached experiment immediately after rupturing the patch.

List EPC5 amplifiers measure voltage and current (3,000 Hz bandwidth), and an HP396A records the signals at 15 ips (5,000 Hz bandwidth). An oscilloscope (model 4094; Nicolet Instrument Corp., Madison, WI) digitizes the signals from tape and sends the digitized traces to a computer (model HP9826; Hewlett-Packard Co., Palo Alto, CA) for analysis; the sampling intervals and any additional filtering of the data appear in the figure legends.

RESULTS

The basic experiment is to patch single cells or small clusters of 2 to 10 cells, which we select for their regular beat. Here we report three results that we obtain under our conditions: (a) The patch has no apparent channel activity (Fig. 1). (b) The patch contains one or more fast Na-conducting channels (Fig. 2) (c) The patch contains a slow Na-conducting channel that, we shall argue, is the Ca channel carrying Na under conditions of zero external Ca (Figs. 3–5).

Fig. 1 summarizes patches that have no apparent channel activity. In this particular experiment, the cell beat spontaneously for over an hour. During this hour, the cell-attached patch was stable but, in thousands of action currents, no obvious single-channel current occurred. Fig. 1 A shows an average of 10 of these apparently blank action currents, and Fig. 1 C shows the time integral of this average. If the patch is a simple capacitor, the action potential relates to the action current by the equation

$$V(t) = \frac{1}{c} \int_o^t i(u)du,$$

where c stands for the capacitance of the patch, $V(t)$ indicates the action potential, and $i(t)$ is the action current.

We check this expectation by measuring $V(t)$ directly.

Fig. 1 B shows the action potential after breaking the patch and switching the amplifier to the whole-cell, current-clamp mode. Ideally, Figs. 1 B and C would be identical; to make the amplitude comparable, let 100 mV = $(1/c)$ 50fC, or $c = 0.5$ pF. Assuming 1 $\mu F/cm^2$ implies a patch area of 50 μm^2. We may also calculate the action current from the action potential by the formula

$$i(t) = c\frac{dV}{dt}.$$

Ideally, Figs. 1 D and A would be identical; from Fig. 1 D, maximum dV/dt is 30 V/s, and from Fig. 1 A, at the same time, $i = 6$ pA. Therefore, $c = 0.2$ pF, which implies a patch area of 20 μm^2. (See the Discussion for an analysis of these estimates.)

In contrast with Fig. 1, which is nearly a pure capacitive action current, the patch in Fig. 2 contains at least three fast Na-conducting channels. Holding the pipette at $V_p = 0$, which is bath potential, the Na channel activity occurs near the peak of the capacitive transient and is difficult to see. Clamping the pipette at positive potentials hyperpolarizes the patch, and the fast Na-conducting channels shift to the right. Fig. 2 A shows an action current for $V_p = 50$ mV; the inward spike (just following the upward capacitive transient) is the Na current; Fig. 2 C shows the same Na current on an expanded time scale.

Although the patch contains at least three fast Na-conducting channels, blanks appear at random throughout a sequence of action currents (Fig. 2 C). We use an average of these blanks to subtract background currents. Fig. 2 D shows the ensemble average of the fast Na-conducting channel (after background subtraction) for $V_p = 50$ mV.
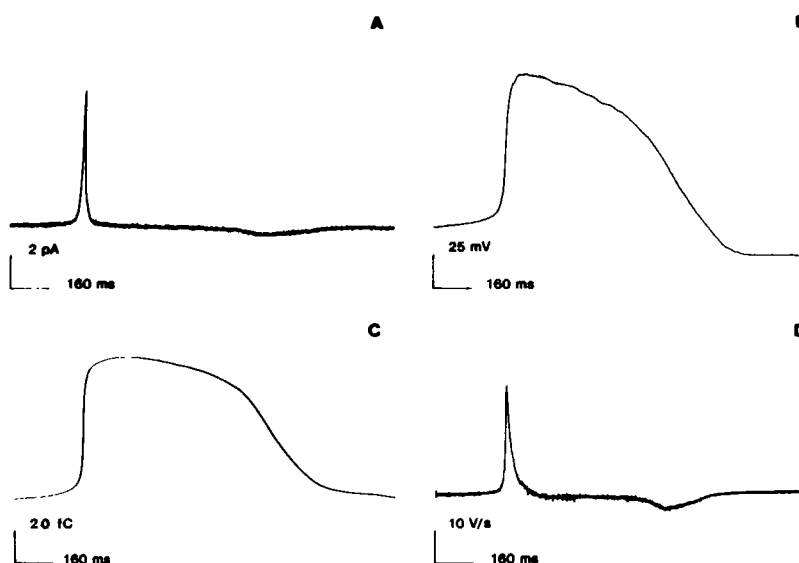

FIGURE 1   Patch action currents and whole-cell action potentials from the same cell. The patch contains no apparent channels. Pipette solution: 133 NaCl, 5 EGTA, 5 Hepes; pH 7.0. Spontaneously beating 7-d chick ventricle at 22°C. $V_p = 0$. (A) Average of 10 blank action currents ($\Delta t = 200$ μs). (B) Whole-cell action potential after breaking the patch ($\Delta t = 200$ μs). (C) Time integral of A; fC = 10^{-15} coulomb. (D) Time derivative of 10 action potentials like B, averaged and digitally filtered at 200 Hz.
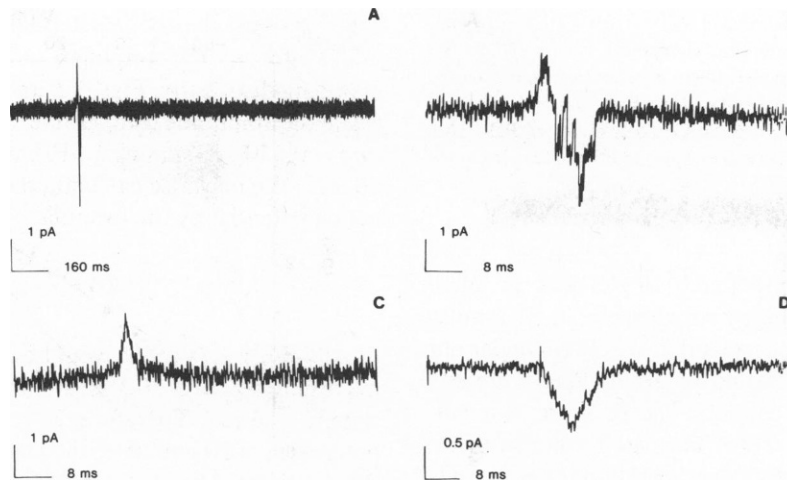
FIGURE 2   Action currents from a cell-attached patch containing fast Na channels. Same conditions as Fig. 1, except $V_p - 50$ mV. The patch contains at least three fast Na channels. $\Delta t - 100$ μs. (*A*) An action current with Na channel activity. (*B*) The same action current on an expanded time scale. (*C*) An action current with no channel activity. (*D*) Average of 36 traces minus the average of 4 blank traces. The four blank traces occurred at random during the 36 action currents.

Hyperpolarizing the patch delays the peak Na current with respect to the peak capacitive transient. It is difficult to obtain data at $V_p = 0$, because the Na current overlaps the capacitive current at that potential. By extrapolation, however, the peak Na current occurs near i_{max} for $V_p = 0$.

The patch in Fig. 3 contains a slow Na-conducting channel, but does not contain fast Na channels. The presence or absence of the two types of Na-conducting channels in any particular patch is uncorrelated with the Na concentration or the type of divalent chelator in the pipette. However, with 10^{-5} gm/ml of TTX in the pipette, we never see the fast Na-conducting channel, although the slow channel is still present. On the other hand, if the

pipette contains Ca (even residual Ca in solutions prepared without Ca but also without Ca chelator) we did not see the slow Na-conducting channel.

Fig. 3 *A* is an example of an action current that contains one slow Na-conducting channel. When the channel is open, the channel current flickers extensively (Fig. 3 *B*). Fig. 3 *C* shows a blank trace, and Fig. 3 *D* shows the ensemble average of the slow Na-conducting channel after background subtraction. The ensemble average of the slow Na-conducting channel at $V_p = 0$ mV peaks late in the action potential during the repolarization phase.

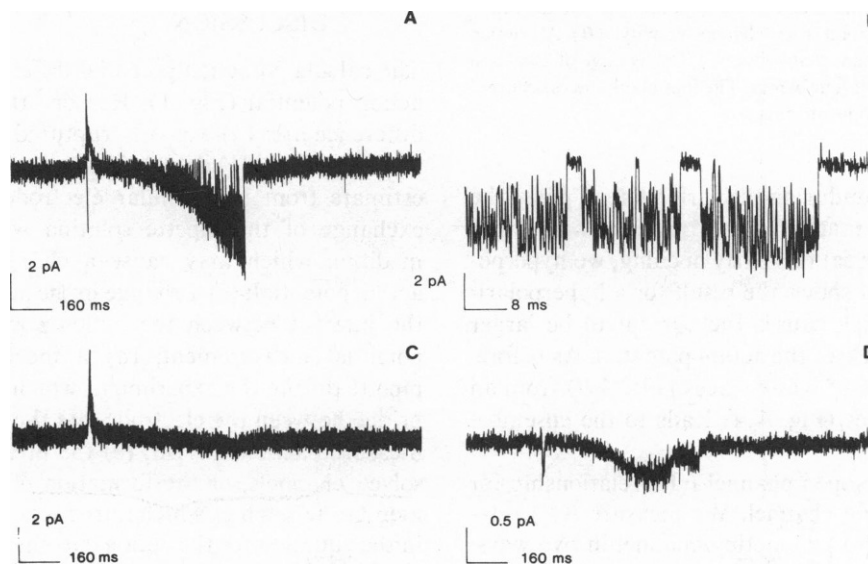The slow Na-conducting channel opens during the foot of the action potential just before the fast capacitive

FIGURE 3   Action currents from a cell-attached patch containing a slow Na conducting channel. Same conditions as Fig. 2, except $V_p - 0$, and the pipette contains 200 NaCl; $\Delta t - 100$ μs. (*A*) An action current with channel activity. (*B*) The same action current on an expanded time scale. (*C*) An action current with no channel activity. (*D*) Average of 40 traces minus the average of 8 blank traces. The eight blanks occurred at random during the 40 action currents.
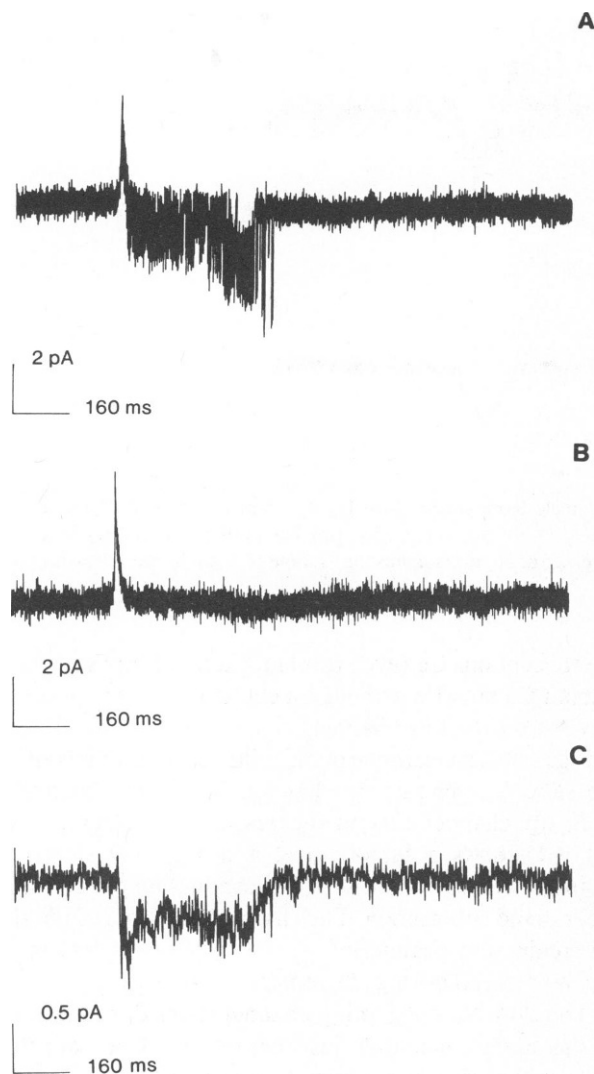
A

2 pA

160 ms

B

2 pA

160 ms

C

0.5 pA

160 ms

FIGURE 4   The same experiment as Fig. 3 except that $V_p = 40$ mV; $\Delta t = 100$ μs. (A) An action current with channel activity. (B) An action current with no apparent channel activity. (C) The average of 20 action currents minus the average of four blanks. The four blank traces occurred at random during the 20 action currents.
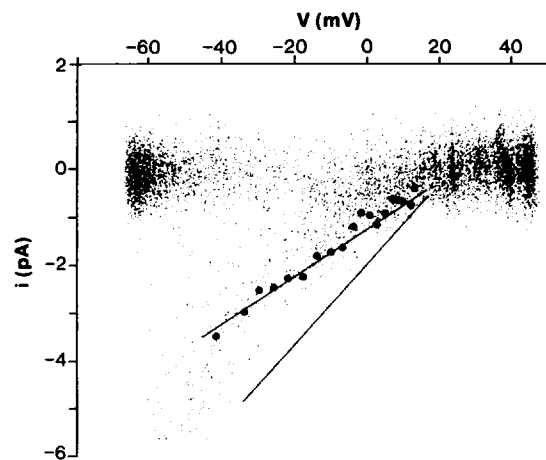
FIGURE 5   The $i(V)$ relationship of the slow Na-conducting channel in 200 Na. Whole-cell action potential vs. a single patch action current (small dots). The patch contains one slow Na-conducting channel. When the channel closes, the dots cluster around $i = 0$; when the channel opens the cloud of dots represent the channel's conductance. The large dots measure the $i(V)$ relationship by averaging open channel currents over brief periods of time during action potentials. A least squares fit through the large dots gives a slope $\gamma = 51.5$ pS and a reverse potential $E = 24.5$ mV. The two lines indicate slopes of 50 p and 90 pS; $\Delta t = 100$ μs for $i(t)$ and $V(t)$.

transient (Fig. 3 A), but during the early plateau phase the patch is near the channel's reversal potential, and the current is small. To reveal this early opening, we hyperpolarize the patch; Fig. 4 shows the result for a hyperpolarization of 40 mV, which causes the current to be larger during the plateau phase of the action potential. As before, subtracting an average of blank traces (Fig. 4 B) from an average of active traces (Fig. 4 A) leads to the ensemble average in Fig. 4 C.

Fig. 5 analyzes the open channel $i(V)$ relationship for the slow Na-conducting channel. We measure $i(V)$ relationship for the slow Na-conducting channel in two ways: (a) the small dots plot the action current against the action potential. The action current contains one active channel. We synchronize the capacitor's current with the maximum rate of rise of the action potential; (b) the large dots

represent an average channel current over 2–5 ms at arbitrary times during an action potential. Since the channel opens randomly, we can obtain channel currents at every potential by examining a sequence of action currents. The potential remains nearly constant during the brief period of the current measurement. The slope of the envelope of the small dots has a value of 90 pS. Using method b the conductance approximates 50 pS and the reversal potential lies near 25 mV.

DISCUSSION

The calculated action potential differs from the measured action potential (Fig. 1). Reasons that may explain this difference are: (a) a poorly ruptured patch, which causes the measured dV/dt maximum to be smaller than the estimate from intracellular electrodes (200 V/s; (b) an exchange of the pipette solution with the intracellular medium, which may cause a change in the whole-cell action potential; (c) a change in the action potential during the interval between the action current and the action potential measurement; (d) a mechanical drift of the pipette during the experiment, which forms a cytoplasmic bridge between the electrode and the cell and changes the measured action current; (e) the presence of small, unresolved channels, or the formation of a leak in the patch membrane, each of which introduces a noncapacitive term in the equation for the action current.

The underestimate of dV/dt maximum causes the calculated value of patch capacitance to be too large. We typically calculate 10–20 μm^2, whereas our pipette resistance measurements, assuming a hemispherical segment of

patch membranes, result in estimates of 5–10 μm^2. The alternative method of calculating patch capacitance introduces even larger errors, because integration of the action current involves the entire shape of the action potential.

The observation of single channels during the action current provides a direct measurement of voltage and time-dependent channel activity during the action potential. Blank action currents allow subtraction of the perturbation due to capacitive transients, unresolved channels, or leaks. The capacitive current normally masks fast Na channel activity, but we may reconstruct this activity by offsetting the patch potential and extrapolating. For the TTX-sensitive channel, the reconstruction of the peak average current shows that the peak occurs near the maximum dV/dt, which helps identify the fast Na-conducting channel we observe in zero Ca with the channel that underlies I_{Na} in normal Ca.

The slow Na-conducting channel blocks in Ca concentrations normally present in solutions made up without Ca ($<10^{-5}$ M). Hess and Tsien (1984) demonstrate that 1.3×10^{-6} M Ca in the bath reduces Na current through Ca channels threefold. The TTX-insensitive, Na-conducting channel opens in long, action-potential length bursts of fast events (1 ms or less) interrupted by complete or partial closures. The extensive flickering and large conductance of the Na-conducting channel are comparable to the results of Hess et al. (submitted for publication): at pH 7.6, rapid transitions in open channel current make the $i(V)$ curve all but impossible to measure; at pH 9, where flickering is less pronounced, the conductance of the channel in 150 mm Na is 85 pS. By using an averaging procedure, we arrive at 50 pS, whereas a direct plot of the flickering current vs. the potential suggests an upper limit of 90 pS (Fig. 5).

Our method of estimating conductance depends on either measuring or calculating the action potential. Fig. 5 uses simultaneous records from two electrodes measuring i and V directly. Using a calculated action potential would be more simple since it involves only one electrode. However, calculating the patch action potential requires a scaling factor and a bias potential to set the absolute units. Furthermore, assuming blank action currents are purely capacitive (Fig. 1 C) usually result in shapes slightly off the measured action potentials (Fig. 1 B). Nevertheless, $i(V)$ plots using calculated action potentials give conductances within ±20% of those we obtain using directly measured action potentials.

On average the channels stay open until the repolarization phase of the action potential (Fig. 3), which may indicate that the channels close primarily because of voltage, and that little of the time-dependent inactivation we expect for Ca channels remains. The shorter duration of the ensemble current in the hyperpolarized patch (Fig. 4) supports this suggestion. Under the hypothesis that the channel we have studied is the Ca channel that has lost its selectivity between divalent and monovalent cations, a diminished time-dependent inactivation might signify that

it is the Ca influx that mediates inactivation under normal conditions, as Mentrard et al. (1984) and Lee et al. (1985) suggest. In our abnormal conditions Na ions (and Ca ions from channels outside the patch) would be less effective in inactivating the channels.

REFERENCES

Almers, W., E. W. McCleskey, and P. T. Palade. 1984. A non-selective cation conductance in frog muscle membrane blocked by micromolar external calcium ions. *J. Physiol. (Lond.).* 270:545–568.

Almers, W., E. W. McCleskey, and P. T. Palade. 1984. Non-selective conductance in calcium channels of frog muscles: calcium selectivity in a single-file pore. *J. Physiol. (Lond.).* 353:585–608.

Cavalie, A., R. Ochi, D. Pelzer, and W. Trautwein. 1983. Elementary currents through Ca^{2+} channels in guinea-pig myocytes. *Pfluegers Arch. Eur. J. Physiol.* 398:284–297.

DeHaan, R. L. 1967. Regulation of spontaneous activity and growth of embryonic chick heart cells in culture. *Dev. Biol.* 16:216–249.

Fischmeister, R., L. J. DeFelice, R. K. Ayer, Jr., R. Levi, and R. L. DeHaan. 1984. Channel currents during spontaneous action potentials in embryonic chick heart cells. The action potential clamp. *Biophys. J.* 46:267–272.

Fukushima, Y., and S. Hagiwara. 1985. Currents carried by monovalent cations through Ca channels in mouse neoplastic B lymphocytes. *J. Physiol. (Lond.).* 357:255–284.

Garnier, D., O. Rougier, Y. M. Gargouil, and E. Coraboeuf. 1969. Analyse electrophysiologigue du plateau des responses myocardiques, mise en evidence d'un courant lent entrant en absence d'ions bivalents. *Pfluegers Arch. Eur. J. Physiol.* 313:321–342.

Hess, P., and R. W. Tsien. 1984. Mechanism of ion permeation through calcium channels. *Nature (Lond.).* 309:453–456.

Hoffman, B. F., and E. E. Suckling. 1956. Effect of several cations on transmembrane potentials of cardiac muscle. *Am. J. Physiol.* 186:317–324.

Kostyuk, P. G., and O. A. Krishtal. 1977a. Separation of sodium and calcium currents in the somatic membrane of mollusc neurones. *J. Physiol. (Lond.).* 270:545–568.

Kostyuk, P. G., and O. A. Krishtal. 1977b. Effects of calcium and calcium-chelating agents on the inward and outward current in the membrane of mollusc neurones. *J. Physiol. (Lond.).* 270:569–580.

Kostyuk, P. G., S. L. Mironov, and Ya. M. Shuba. 1983. Two ion-selecting filters in the calcium channel of the somatic membrane of the mollusc neurones. *J. Membr. Biol.* 76:83–83.

Lee, K. S., and R. W. Tsien. 1984. High selectivity of calcium channels in single dialyzed heart cells of the guinea pig. *J. Physiol. (Lond.).* 354:253–272.

Lee, K. S., E. Marban, and R. W. Tsien. 1985. Inactivation of Ca channels in mammalian heart cells: joint dependence on membrane potential and intracellular Ca. *J. Physiol. (Lond.).* 364:395–411.

Levi, R., and L. J. DeFelice. 1984. International Union of Pure and Applied Biophysics, Bristol, UK. 280.

Mentrard, D., G. Vassort, and R. Fischmeister. 1984. Calcium-mediated inactivation of the conductance in cesium loaded frog heart cells. *J. Gen. Physiol.* 83:105–131.

Rougier, O., G. Vassort, D. Garnier, Y. M. Gargouil, and E. Coraboeuf. 1969. Existence and role of a slow inward current during the frog atrial action potential. *Pfluegers Arch. Eur. J. Physiol.* 308:91–110.